ELSEVIER

Journal of Chromatography A, 865 (1999) 111–122

JOURNAL OF CHROMATOGRAPHY A

www.elsevier.com/locate/chroma

Study of hydrophobic interaction adsorption of bovine serum albumin under overloaded conditions using flow microcalorimetry

Maria A. Esquibel-King[a], Ana Cristina Dias-Cabral[b], Joao A. Queiroz[b], Neville G. Pinto[a,*]

[a]*Department of Chemical Engineering, University of Cincinnati, Cincinnati, OH 45221, USA*
[b]*Department of Chemistry, Universidade de Beira Interior, 6200 Covilha, Portugal*

Abstract

The adsorption behavior of bovine serum albumin (BSA) on a Sepharose based hydrophobic interaction support has been studied. Flow microcalorimetry has been used to determine the heat of adsorption under overloaded chromatographic conditions. These data have been complemented with capacity factor and isotherm measurements to provide insight on the mechanisms of adsorption. The heat of adsorption data have confirmed that the hydrophobic interaction adsorption of BSA under linear isotherm conditions is driven by entropy changes. Under overloaded (non-linear) conditions, however, it has been shown that the changes in enthalpy can drive adsorption; this behavior is not evident from analyses of capacity factor data. It is postulated that for BSA adsorption on the Sepharose derivative of interest, attractive force interactions between adsorbed protein molecules drive the adsorption process under overloaded conditions in a high $(NH_4)_2SO_4$ environment. It is further postulated that these interactions are due to a change in confirmation of the adsorbed protein under these conditions.

Keywords: Hydrophobic interaction chromatography; Flow microcalorimetry; Thermodynamic parameters; Albumin; Proteins

1. Introduction

Hydrophobic interaction chromatography (HIC) is a separation technique that has recently gained much attention for the downstream purification of biomolecules. Reports in the literature include the successful purification of therapeutic proteins, removal of viruses from human plasma, and the isolation of bacterial enzymes [1–4]. In HIC, interactions between hydrophobic moieties on the adsorbate (i.e. biomolecule) and an insoluble, immobilized hydrophobic ligand on the support effect separations. It is believed that the increase in entropy originating from the release of water molecules from the surface provides the main driving force for adsorption [5].

Linear HIC has been used as a tool for investigating the mechanisms underlying the hydrophobic interaction process [6–10]. One approach exploits the well known Van 't Hoff relation. Horváth and co-workers [6,7] have used this relation in a study of the HIC retention behavior of dansyl amino acids on Spherogel, SynChropak propyl, and TSK-Gel butyl-NPR supports. They found that for these systems the Van 't Hoff plot was non-linear. Postulating that this non-linearity originated from the dependence of the standard-state enthalpy change of adsorption on temperature, they corrected for this using Kirchoff's

*Corresponding author. Tel.: +1-513-556-2761; fax: +1-513-556-3473.

0021-9673/99/$ – see front matter
PII: S0021-9673(99)01118-8

relations. With this correction the capacity factor (k') is related to temperature (T) by the equation:

$$\ln k' = \frac{\Delta C_P^0}{R}\left(\frac{T_H}{T} - \ln\frac{T_S}{T} - 1\right) + \ln\phi \quad (1)$$

where ΔC_p^0 is the standard state heat capacity change; T_H and T_S are the reference temperatures at which ΔH^0 and ΔS^0 are zero; and ϕ is the phase ratio.

Using Eq. (1), Horváth and co-workers concluded that the adsorption of dansyl amino acids on the HIC supports studied was entropically driven at low temperatures and enthalpically driven at higher temperatures.

Perkins et al. [10] proposed an alternative approach based on the Preferential Interaction model. This model describes protein retention in HIC as a function of the stationary-phase ligand hydrophobicity and mobile phase composition. It focuses on the interactions of solutes with the proteins by making use of the preferential interaction coefficient. The model, when applied to linear chromatography, provides a convenient interpretation of the effects of solutes on the adsorption process. For the retention of a protein (2) in the presence of a salt (3) and a solvent (1), the governing equation is:

$$\ln k' = \ln m_3 \cdot \left(\frac{\Delta\nu_+ - \Delta\nu_-}{g}\right) - m_3 \cdot \left(\frac{n \cdot \Delta\nu_1}{m_1 g}\right) + C \quad (2)$$

where $\Delta\nu_i$, is the stoichiometric weighted change in the number of moles of the species i in the local region of the products (protein–ligand complex) and reactants (protein in solution and ligand on the surface) following adsorption: m_3 is the salt concentration; and n, and m_1 are, respectively, the total number of ions associated with the electrolyte, and the molal concentration of water. The value for g is tabulated for activity coefficients as a functions of salt concentration. The $+$ and $-$ refer to cations and anions of the electrolyte.

By plotting Eq. (2), the number of water molecules released ($\Delta\nu_1$) and the change in the binding of ions ($\Delta\nu_+ - \Delta\nu_-$) can be estimated. Perkins et al. [10] applied this equation to a number of HIC systems, and reported that the release of water molecules (100–200) was significantly more than the release of salt ions (0.5–3). This result is consistent with the commonly accepted idea that in HIC protein adsorption is an entropically driven process.

In this article we describe the adsorption behavior of bovine serum albumine (BSA) on a Sepharose-based hydrophobic interaction support in both the linear and non-linear regions of the isotherm. We have reported heat of adsorption data obtained as a function of salt concentration and temperature. Using these data in conjunction with adsorption isotherms. we provide new insight on the complexity of the adsorption process.

We have also analyzed linear HIC data with Van't Hoff plots. By comparing standard-state heats of adsorption obtained with these plots with heat of adsorption data from the flow microcalorimetry, we have studied the validity of using Van't Hoff analysis for obtaining energetic data. Finally, we have analyzed linear retention data with the Preferential Interaction model to investigate the potential of using data obtained in the linear regime to non-linear applications.

2. Experimental

2.1. Materials and apparatus

BSA was chosen as the probe protein. It was purchased from Sigma (St. Louis, MO, USA), and used without further purification. BSA is a globular ellipsoid (14×4×4 nm), with a molecular mass of 69 000, and an isoelectric point (pI) of 4.7 [11]. The HIC support (Fig. 1) was a Sepharose derivative synthesized by covalent immobilization of the ligand 1,4-butandiol diglycidyl ether on Sepharose CL-6B purchased from Pharmacia Biotech Europe. The synthesis procedure has been described in detail elsewhere [3]. Briefly, 1,3-butadiene diepoxide is coupled to Sepharose CL-6B activated gel. The derivatized gel is then treated with 1.0 *M* sodium hydroxide overnight at room temperature to inactivate free epoxy groups.

A 0.1 *M* sodium phosphate buffer, which consisted of a mixture of equimolar dibasic and monobasic sodium phosphate, was used for all the experiments. Ammonium sulfate was used as the modulator.

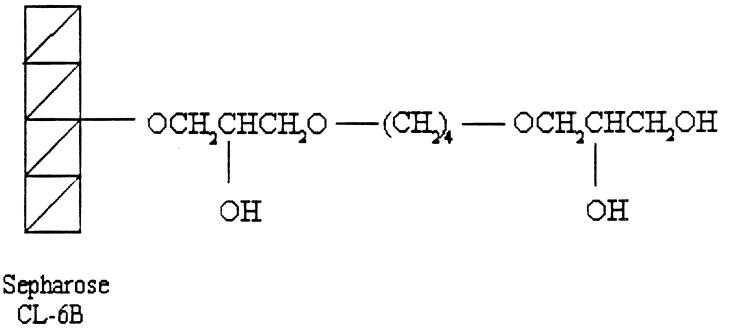

Fig. 1. Structure of Epoxy-$(CH_2)_4$-Sepharose derivative.

2.2. Flow microcalorimetry

The heat of adsorption was measured using a Flow MicroCalorimeter (FMC). The FMC C (Gilson Instruments, Westerville, OH, USA) operates isothermally, and has a precision fluid delivery system (syringe micropumps), a vacuum system to pre-evacuate a sample in situ, and a block heater and monitor to control cell temperatures. Calibration is via electrical energy dissipation in the cell under static or flowing conditions.

The FMC is operated similar to a liquid chromatograph with the cell (0.171 ml) in place of the column. The FMC cell is first properly packed with a specified amount of the dried adsorbent. Deionized (DI) water is then introduced until equilibration; this wetting process takes at least 48 h. Following equilibration with DI water, buffered solution is introduced at 3.33 ml h^{-1} and the system is re-equilibrated. Protein sample is then injected through a sample loop (91 μl) and the heat of adsorption is measured through thermistors located in the cell. The effluent from the calorimeter was collected during the adsorption experiments, and its protein concentration determined with a Shimadzu UV-160 Spectrophotometer (Kyoto, Japan) at a wavelength of 280 km. From a mass balance, the amount of protein adsorbed was calculated. At the end of each heat of adsorption measurement, the protein was removed from the cell by passing the 10 m*M* sodium phosphate buffer.

2.3. Isotherm measurements

BSA adsorption isotherms were measured at different ammonium sulfate concentrations at room temperature (23°C) using a batch method. The adsorbent was first weighted into test tubes. then a measured volume of protein solution at known salt and protein concentrations at pH 7 was added. The test tubes were sealed with Parafilm and placed in an orbital shaker (Model 4518, Forma Scientific, OH, USA) for 24 h at 230 rpm. After equilibration, the slurry solution was allowed to settle for 30 min and and a sample of the supernatant was removed with a filter (0.45 μm) syringe. The sample was then analyzed with a UV spectrophotometer at 280 nm. The equilibrium distribution was calculated from a mass balance.

2.4. Isocratic elutions

The capacity factor measurements were made on a 4.1×1 cm I.D. column at 23, 30 and 35°C. The column was equilibrated with 10 *M* phosphate buffer at a pH of 7, with different concentrations of ammonium sulfate at a flow-rate of 0.24 ml min^{-1}. Elution times (t_r) were obtained by injecting 100 μl of 2.0±0.02 mg ml^{-1} BSA. Following the elution, the column was washed with 10 m*M* phosphate buffer (pH 7). The response was monitored with a UV detector at 280 nm.

3. Results and discussion

3.1. Van 't Hoff analysis

Retention data obtained for BSA on the Epoxy-$(CH_2)_4$-Sepharose support are shown in Fig. 2.

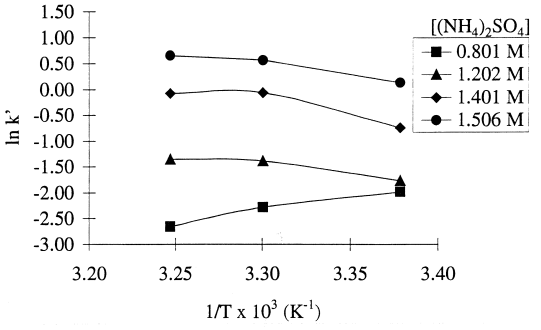

Fig. 2. Van't Hoff plot for the retention of BSA on epoxy-$(CH_2)_4$-Sepharose.

Measurements were made at four concentrations of $(NH_4)_2SO_4$. It is observed that at every temperature the capacity factor decreases with decreasing $(NH_4)_2SO_4$ concentration, as is to be expected for HIC.

The data in Fig. 2 are plotted on a Van't Hoff plot ($\ln k'$ vs. $1/T$). It is seen that the relationship is non-linear, as is commonly observed for HIC. Following Horváth and co-workers approach [6,7] of incorporating the dependence of ΔH^0 on temperature, Eq. (1), known as the logarithmic equation (L), was used to characterize the data in Fig. 2. Horváth and co-workers have also proposed a refinement that corrects for the variation of ΔC_p^0 with temperature. This gives the equation:

$$\ln k' = a + \frac{b}{T} + \frac{c}{T^2} + \ln \phi \quad (3)$$

This equation known as the quadratic equation (Q), was also used to characterize the data in Fig. 2. The results are shown in Table 1.

Both ΔH^0 and ΔS^0 were found to have a strong dependence on temperature and salt concentration. Also, the values obtained using the logarithmic (L) and quadratic (Q) equations were found to be in good agreement: this is consistent with the results of Horváth and co-workers [6,7], and indicates that temperature variation of ΔC_p^0 is not significant. In most cases, at the lower temperatures the values of ΔH^0 and ΔS^0 are positive and as the temperature increases these values decrease or become increasingly negative. This suggests that retention in HIC is entropically driven at low temperatures and enthalpically driven at higher temperatures, which is in agreement with previous results. It should also be noted that the standard-state enthalpy of adsorption ΔH^0 is relatively small (-2 to 27 cal mol^{-1}), which indicates weak enthalpic effects in all cases.

3.2. Preferential interaction analysis

The HIC retention data were also analyzed with the preferential interaction model described earlier. Eq. (2) was fitted to the experimental data using

Table 1
Thermodynamic quantities for the retention of BSA on epoxy-$(CH_2)_4$-Sepharose as evaluated by fitting data to the logarithmic equation, Eq. (1), (L) and the quadratic equation, Eq. (3), (Q)

Temperature (°C)	$[(NH_4)_2SO_4]$ (M)	ΔH^0 (cal mol^{-1})		ΔS^0 (cal mol^{-1})	
		L	Q	L	Q
23	0.801	−2.66	−2.61	−8.02	−7.61
30		−11.97	−12.09	−39.11	−39.25
35		−18.62	−18.59	−60.88	−60.55
23	1.202	14.20	14.26	49.37	49.85
30		4.64	4.53	17.46	17.37
35		−2.18	−2.15	−4.88	−4.49
23	1.401	26.69	26.94	93.92	94.76
30		6.43	6.31	26.25	25.87
35		−8.05	−7.85	−21.13	−20.48
23	1.506	15.01	15.12	56.14	56.52
30		6.37	6.32	27.28	27.15
35		0.20	0.28	7.08	7.38

Table 2
Estimate of the release of water molecules and salt ions for adsorption of BSA on epoxy$(CH_2)_4$-Sepharose

Protein	Temp. (°C)	$\left(\frac{-n\cdot\Delta\nu_1}{m_1\cdot g}\right)$	$\left(\frac{\Delta\nu_+ + \Delta\nu_-}{g}\right)$	c	$-\Delta\nu_1$	$-(\Delta\nu_+ + \Delta\nu_-)$
BSA	23	8.88	−0.19	−3.78	262.82	0.309
BSA	30	9.2	−0.08	−3.22	271.47	0.136
BSA	35	9.1	−0.17	−3.33	269.41	0.272

non-linear least squares fitting software [9]. Table 2 lists the parameters obtained; for the system used the values for n, m_1, and g in Eq. (2) are 3, 55.15, and 1.6, respectively. In Table 2, $\Delta\nu_1$ corresponds to the change in the number of bound water molecules, and $(\Delta\nu_+ - \Delta\nu_-)$, is the change in bound salt ions on adsorption. A negative value indicates a net release from the surface. From the results, the adsorption of BSA is accompanied by a large release of water molecules (263–271), and a relatively small number of ions (0.14–0.31). These results support an entropically driven process, in which the release of a large number of ordered water molecules provides the driving force for adsorption. The results also lead to the conclusion that ion-exchange is not a significant mechanism. These conclusions are consistent with results reported in the literature for other HIC systems [5,10].

3.3. Heats of adsorption

Based on the results from the Van't Hoff and preferential interaction analyses, it is to be expected that heat of adsorption measured by the FMC will be small and/or endothermic, at least in the linear region of the isotherm. Shown in Fig. 3 are the observed heats at 23°C and 0.6 and 0.8 M salt concentrations; these data are reported as a function of the surface concentration of the protein. The heats of adsorption in Fig. 3 were calculated from FMC signals that are typically represented in Fig. 4. Because the FMC is operated under conditions such that $\Delta H_{ads} = Q_{ads}$, the data are reported in terms of the enthalpy change of adsorption.

As was expected, at lower protein surface concentrations no significant enthalpy change of adsorption was observed. This confirms the conclusions of the Van't Hoff and preferential interaction analyses that the adsorption is entropically driven in linear HIC. At higher surface concentrations, however, significant endothermic heats were obtained. As can be seen in Fig. 3, there is a threshold surface concentration, at each salt condition, above which the enthalpy change of adsorption rapidly rises to a maximum and then gradually decreases as the surface concentrations is further increased. It is useful to compare the measured ΔH_{ads} in Fig. 3 with the standard-state enthalpy change calculated from the Van't Hoff plot (Table 1) at the common condition of 23°C and 0.8 M $(NH_4)_2SO_4$. It is seen that while the latter predicts a small negative (~ -2 cal mol^{-1}; 1 cal = 4.1843) standard-state change in enthalpy, the experimental ΔH_{ads} are positive and much larger in magnitude (200–250 cal mol^{-1}). The substantial positive changes in ΔH_{ads} suggest the presence of significant repulsive interactions and/or a change in protein confirmation or orientation at these conditions. It is worth noting that the directly measured ΔH_{ads} are obtained at conditions that exist in a chromatographic column (as opposed to standard-state values), and are therefore representative of the thermodynamics of the actual process. It is also important to note, however, that the FMC data do confirm that the adsorption is entropically driven even at non-linear protein loadings.

The heats of adsorption was also measured at higher $(NH_4)_2SO_4$ concentrations at 23°C. Shown in Figs. 5 and 6 are the heats of adsorption at 1.5 and 1.0 M $(NH_4)_2SO_4$, respectively. What is most significantly different in these figures, in comparison to the lower salt concentrations, is the presence of exothermic peaks at higher protein loadings. A typical FMC signal for this case is shown in Fig. 7. Two peaks, an endothermic peak followed by an exothermic peak, are observed. These peaks suggest the presence of at least two processes: and entropically driven process at lower protein loadings ($\sim < 2$ mmol kg^{-1}), and an enthalpically driven process at

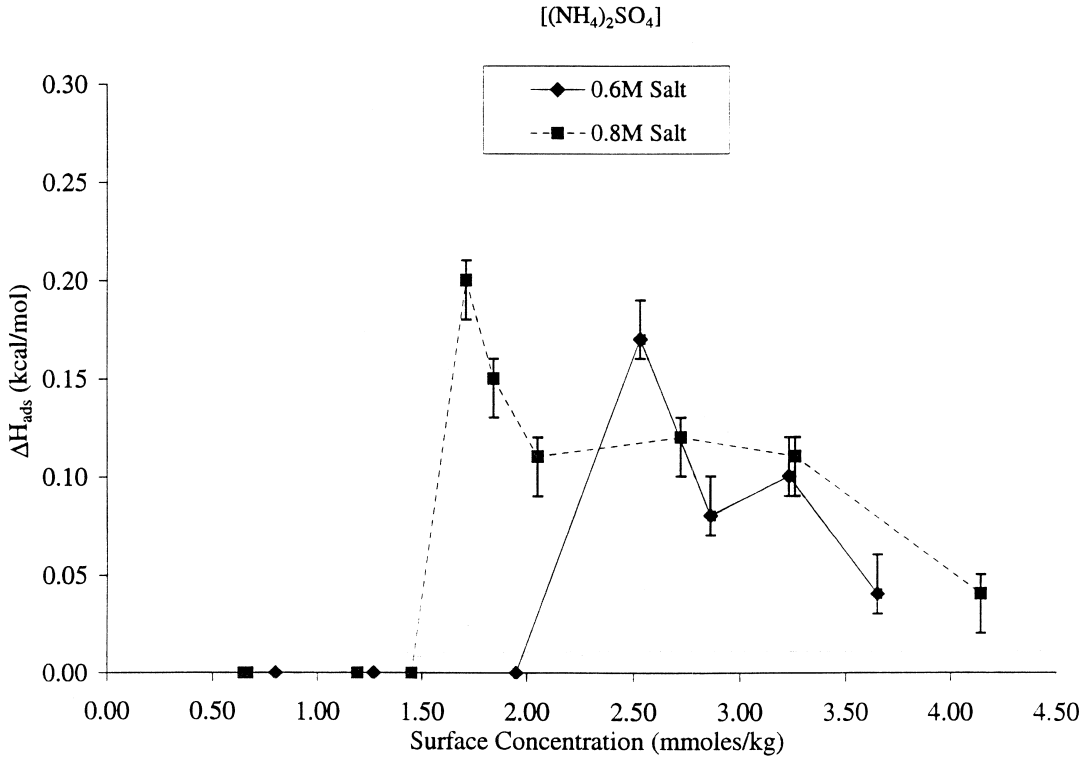

Fig. 3. Heat of adsorption of BSA on epoxy-$(CH_2)_4$-Sepharose at low salt concentrations ($T=23$°C, pH 7.0).

higher loadings. These processes may be occurring simultaneously with the entropically driven process lasting over a shorter period. they may be partially overlapping, or they may be occurring in sequence.

One test that is often used to establish whether peaks overlap is peak symmetry. The peak width at half peak height can be compared for the endothermic peak in the absence of the exothermic peak (lower protein concentration) and in the presence of the exothermic peak (higher protein concentration). If the peak widths are significantly different, this indicates that exothermic and the endothermic peaks overlap. Shown in Table 3 are the peak widths at half peak height for the endothermic peak in the presence and absence of the exothermic peak. Clearly, the endothermic peak is substantially sharpened by the exothermic peak, indicating an overlap of the two peaks.

In order to separate the two signals the peaks were de-convoluted using Table Curve 2D software [12]. Fig. 8 illustrates a case. It can be seen that the analysis suggests that the exothermic peak completely overlaps the endothermic peak. That is, at high protein loadings the process is driven both by enthalpy and entropy. One possible explanation is that multi-layer formation; i.e., enthalpically driven protein on protein adsorption is occurring simultaneously with the release of water from the surface. This possibility will be discussed in more detail after the adsorption isotherms have been presented.

The de-convoluted values of the exothermic and endothermic heats of adsorption at all protein surface concentrations studied at 1.5 M $(NH_4)_2SO_4$ are shown in Fig. 5. While the de-convoluted data have essentially the same type of concentration dependence as the original data, the magnitudes of the both the exothermic and endothermic heat are significantly higher when de-convoluted. In fact, the magnitude of the de-convoluted exothermic heat is comparable to the endothermic heat observed: for example at 1.5 M $(NH_4)_2SO_4$ the maximum exothermic heat is approximately 900 (cal mol^{-1})

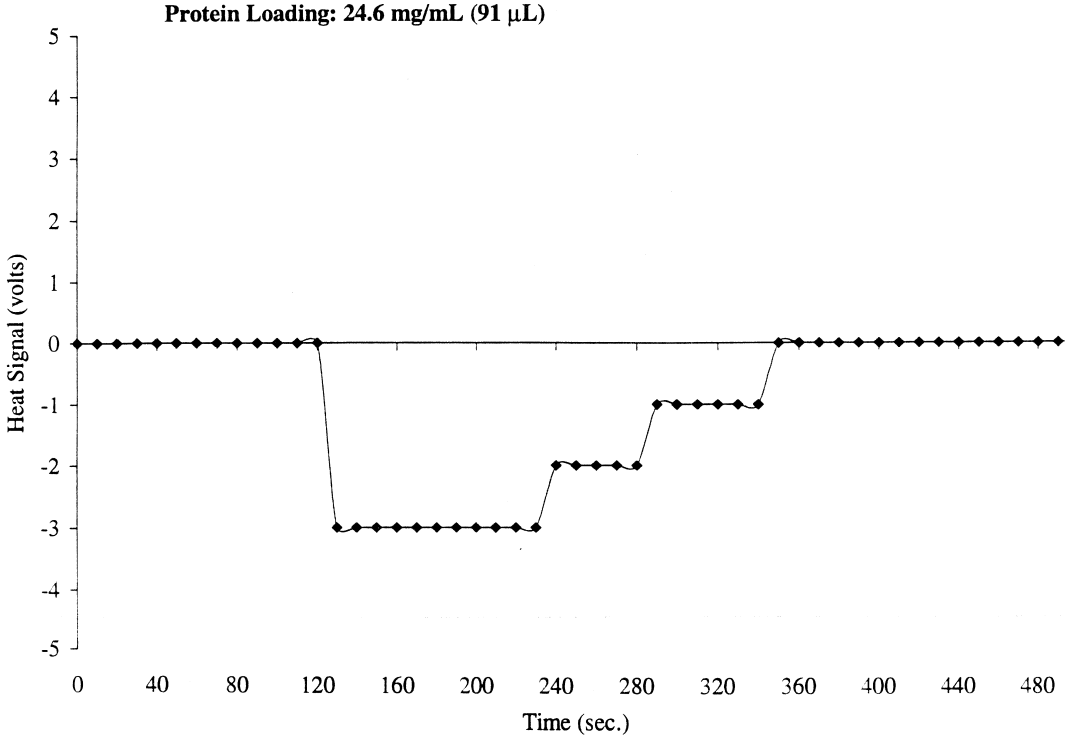

Fig. 4. Typical heat signal for BSA adsorption epoxy-$(CH_2)_4$-Sepharose at 0.8 *M* $(NH_4)_2SO_4$ (T=23°C, pH 7.0).

while the maximum endothermic heat is approximately 1300 (cal mol^{-1}). This emphasizes the importance of the enthalpic driving force under overloaded conditions. The presence of this significant effect was not evident from the Van't Hoff or preferential interaction analysis, for the simple reason that this effect is not present at lower protein coverage, as is clear in Figs. 5 and 6.

An interesting observation is made if the endothermic data in Fig. 5 and 6 are compared to the corresponding data in Fig. 3. Based on the Van't Hoff and preferential interaction model, and the data in Fig. 3, it is reasonable to assume that the endothermic heat at low protein concentrations is zero or small (data could not be obtained at very low concentrations on the FMC because of limits imposed by sensitivity of the concentration detector). This would imply there is a maximum similar to that observed in Fig. 3 for the higher salt concentrations (Figs. 5 and 6). This maximum appears to increase with increasing salt concentrations, and the threshold for the rapid rise appears to occur earlier at higher concentrations. This trend is consistent with the explanation proposed earlier that the endothermic heat originates from increasing repulsive interactions as surface coverage increases and/or a change in confirmation or orientation of the adsorbed protein. It is to be expected that at higher $(NH_4)_2SO_4$ concentrations, the entropic driving force is enhanced. Thus, more energy is available to overcome enthalpically unfavorable processes, and this can be achieved at a lower surface coverage.

Valuable insight is also obtained by qualitatively correlating the ΔH_{ads} data to adsorption isotherms. Shown in Fig. 9 are the adsorption isotherms as a function of salt concentration at 23°C. As is expected for an HIC support, as the salt concentration increases the amount that is adsorbed increases. At all salt concentrations, with increasing protein liquid concentrations an increase from zero capacity to a well defined plateau region is observed. This plateau is followed, at least for the two higher salt concentrations, by a region of rapidly increasing capacity, indicating the formation of bi- or multi-layers of

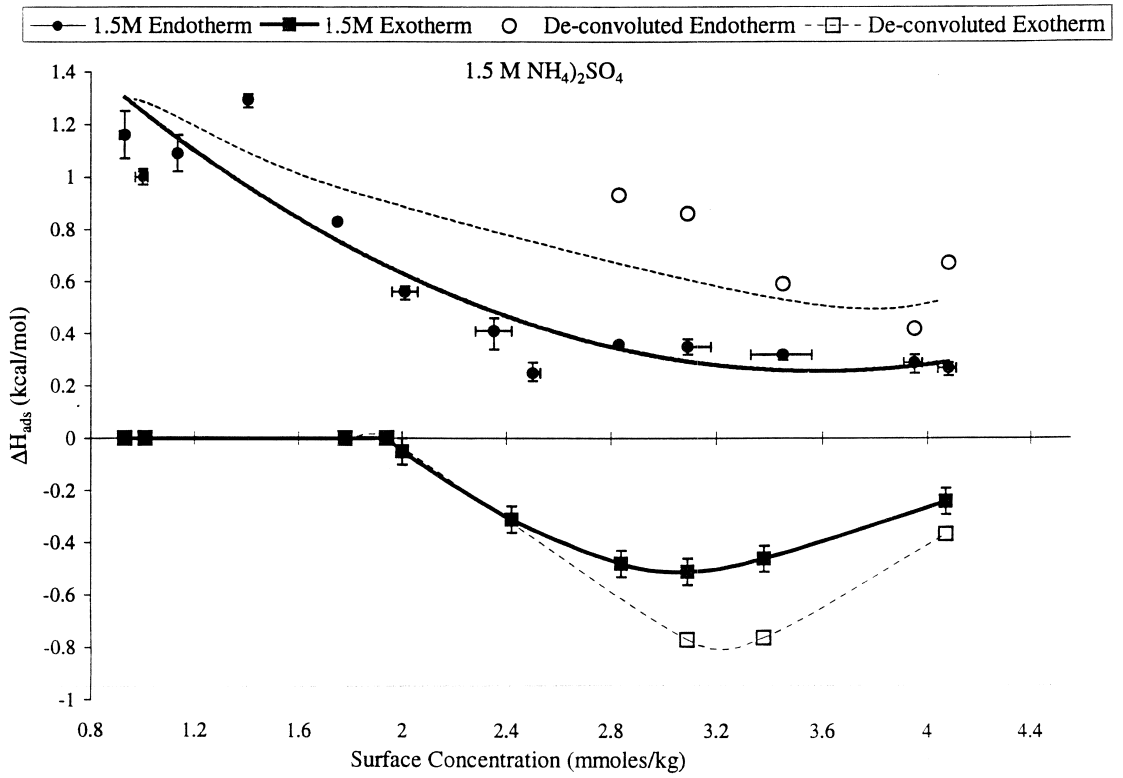

Fig. 5. Heat of Adsorption of BSA on Epoxy-$(CH_2)_4$-Sepharose at 1.5 *M* $(NH_4)_2SO_4$ (T=23°C, pH 7.0).

BSA on the surface, or a reorientation and/or reconfiguration of the adsorbed protein. It is interesting to note that the start of this region of increasing capacity occurs for both salt concentrations, between approximately 1.6 to 1.9 (mmol kg^{-1}) protein surface concentration, which corresponds closely to the surface concentration at which the exothermic heat is first observed (Figs. 5 and 6). This strongly suggests that adsorption beyond the first plateau is driven by enthalpy, very possibly originating from attractive force interactions between BSA molecules.

In a study of the adsorption behavior of human plasma albumin on a hydrophobic polystyrene support. Norde and Lyklema [13] obtained isotherms similar in shape to the higher salt concentrations isotherms shown in Fig. 9. They postulated that the increase in capacity beyond the plateau was due to re-orientation or conformational alterations in the adsorbed molecules, rather than due to bi-layer formation. They proposed that the mechanism of adsorption in this region differs from that at lower solution concentrations. This explanation appears to be valid for the present case as well.

The dependence of the exothermic ΔH_{ads} on the surface concentration in Fig. 5 and 6 shows a decrease to a sharp minimum (maximum exothermic heat) followed by an increase as the surface concentration increases further. This behavior appears to be consistent with re-orientation and/or a change in confirmation rather than multi-layer formation. If multi-layer formation was driving the increase in capacity, the sharp minimum observed in the exothermic ΔH_{ads} would only be present if the adsorption capacity was limited by the pore size soon after the first plateau is reached. However, since Sepharose has a very open gel structure, pore size is unlikely to be of consequence until a significant number of BSA layers have formed, and the minimum on the ΔH_{ads} exothermic curve would expected to be broad in this case.

The sharp minimum can, however, be justified if re-orientation and/or reconfirmation is the cause for

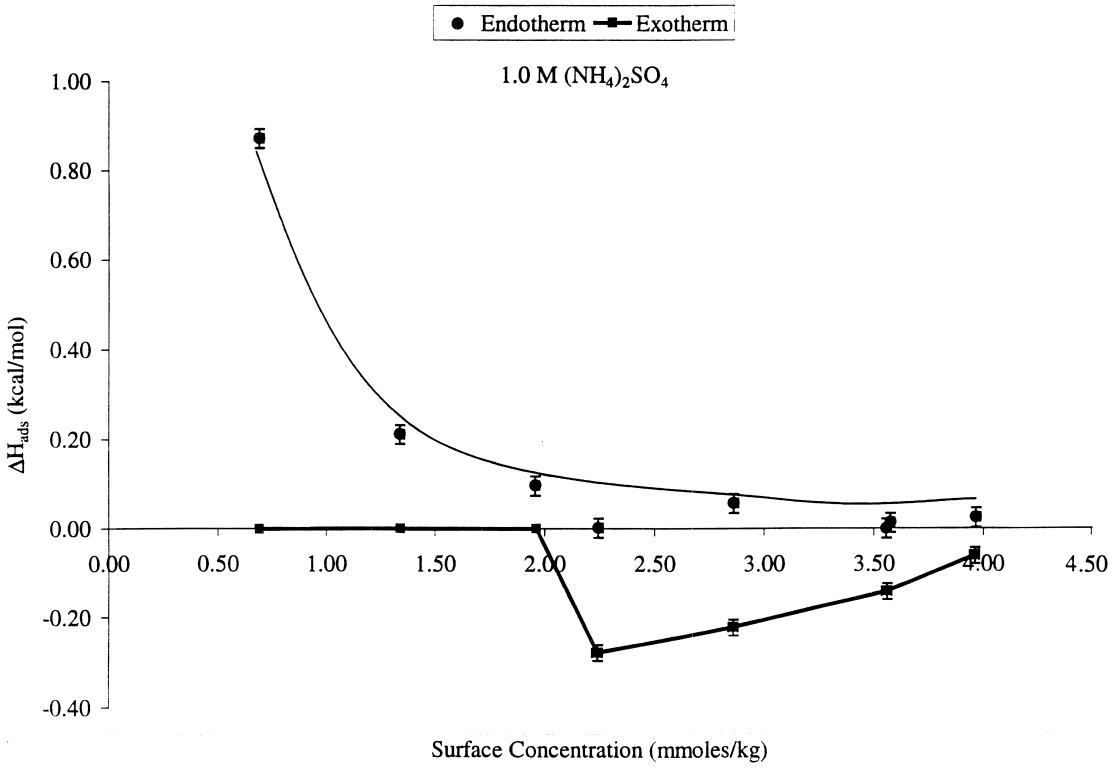

Fig. 6. Heat of adsorption of BSA on Epoxy-$(CH_2)_4$-Sepharose at 1.0 *M* $(NH_4)_2SO_4$ (T=23°C, pH 7.0).

the increased capacity beyond the plateau. In this case, re-orientation/reconfiguration of the adsorbed molecules establishes a new, enhanced monolayer capacity. The process of reorientation/reconfiguration is enthalpically driven due to attractive interactions between adsorbed molecules at high surface coverages. The exothermic heat of adsorption would increase when reorientation/reconfirmation first occurs and would decrease as the new monolayer capacity is reached. Since this capacity is likely to be quite close to the plateau capacities observed in the isotherm, the exothermic ΔH_{ads} can be expected to give a sharp minimum, as observed. It should be noted that it was unfortunately not possible to measure the equilibrium isotherm beyond 70 (mg ml^{-1}) of BSA liquid concentration in Fig. 9, because of experimental difficulties with solubilizing the protein. Thus, the existence of a second plateau for each isotherm could not be confirmed. However, because the FMC data were obtained in what is equivalent to an isocratic elution mode, higher surface concentrations could be achieved with this method, and the approach of both the exothermic and endothermic ΔH_{ads} to zero at higher surface concentrations strongly suggests the existence of a second saturation plateau.

Re-orientation and/or reconfirmation of adsorbed BSA at high surface coverage is also apparently influenced by the salt concentration. If it were not, exothermic heats should have been observed in Fig. 3. Clearly, this was not the case, even though the surface coverage exceeded the 1.6 to 1.9 (mmol kg^{-1}) range at which exothermic heats were first observed at the higher salt concentrations. The salt can influence orientation of the adsorbed BSA through electrostatic shielding. However, the difference in this influence between the lower concentrations (0.6 and 0.8 *M*) and higher concentrations (1.0 and 1.5 *M*) is unlikely to be significant, since even the lowest salt concentration used is substantially concentrated, and should give virtually the same electrostatic shielding as the highest concentration.

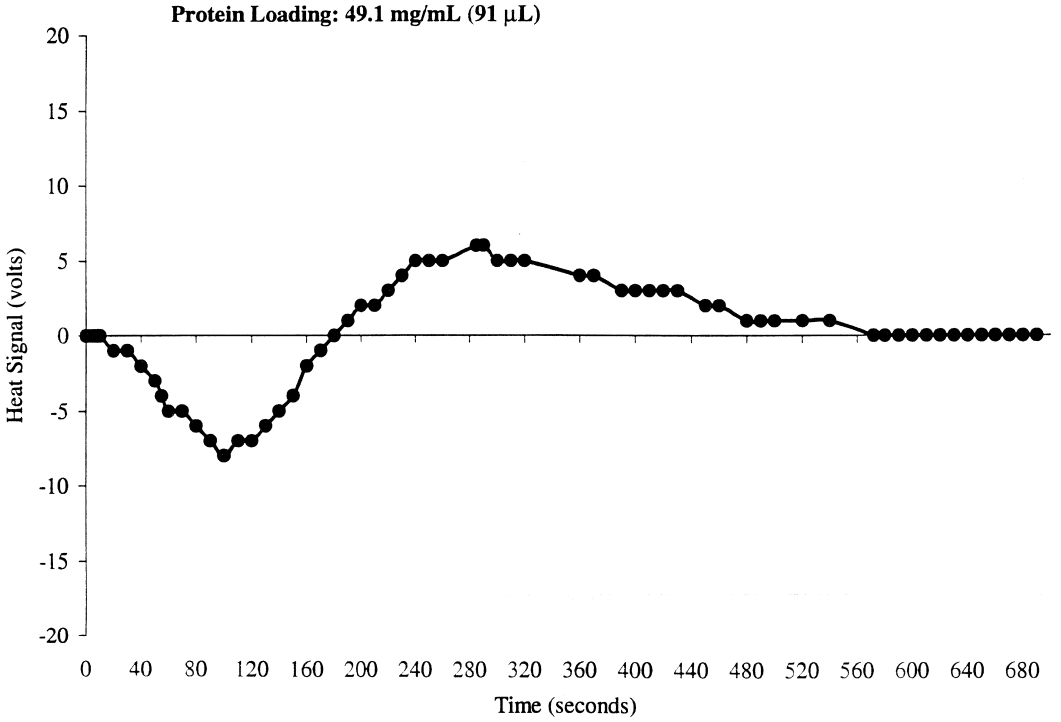

Fig. 7. Typical FMC heat signal for the adsorption of BSA on epoxy-$(CH_2)_4$-Sepharose (T= 23°C, pH 7.0; time scale adjusted for a dead time of 187 s).

What is more likely is that the salt concentration affects protein confirmation differently at the lower and higher salt concentrations. The different confirmations result in exothermic (attractive) interactions dominating in one case and endothermic (repulsive) interactions dominating in the other.

Table 3
Peak widths of endothermic peaks at 1/2 height at 23°C, pH 7, and 1.5 M $[(NH_4)_2SO_4]$

FMC heat signal	Surface concentration (mmol kg^{-1})	Peak width (s)
No exothermic peak	0.91	84
	1.97	91
	2.04	88
Exothermic peak present	2.53	77
	2.84	76
	3.98	59

4. Conclusions

It has been demonstrated that heat of adsorption measurements using FMC provides valuable data on the adsorption behavior of proteins in HIC. These data have confirmed the conclusions reached based on the analyses of capacity factor data, that adsorption under linear conditions in HIC is entropically driven by the release of water molecules. However, it has been shown that conclusions reached under linear conditions cannot in general be extrapolated to non-linear (overloaded) chromatography. In particular, conditions can exist where the adsorption is enthalpically driven at high surface coverage while it is entropically driven at lower coverage. Furthermore, it has been shown that standard-state enthalpy of adsorption obtained with a Van't Hoff type analysis do not satisfactorily correspond to the enthalpy of adsorption under overloaded chromatographic conditions. For the particular case studied.

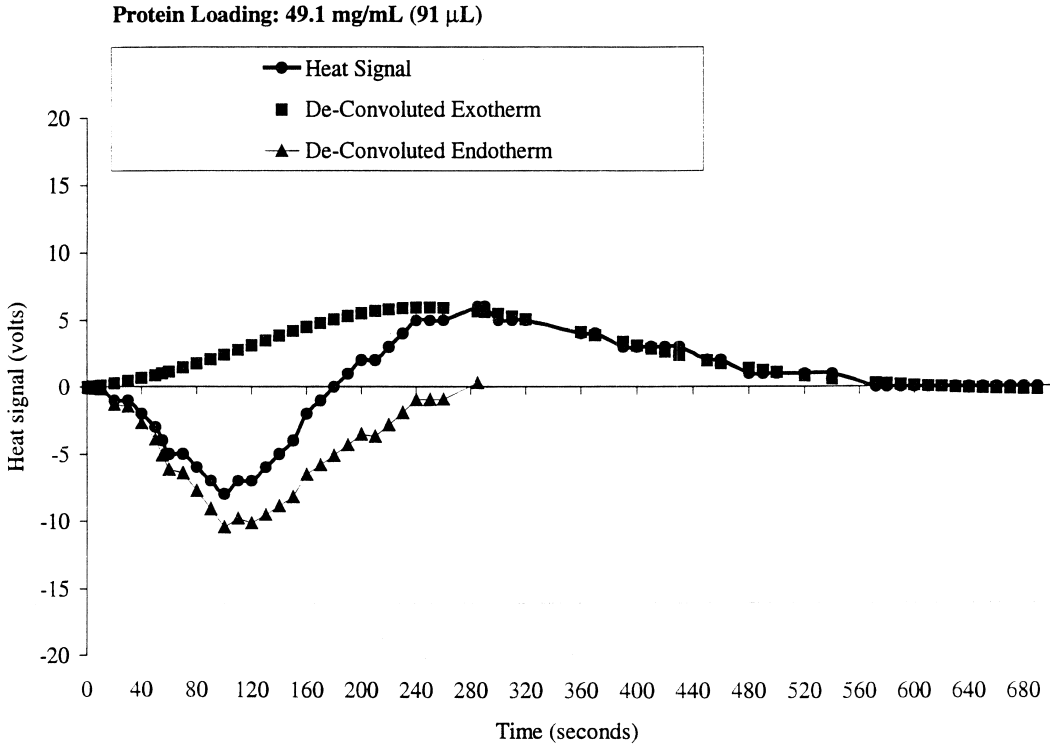

Fig. 8. De-convolution of heat signal for the adsorption of BSA on epoxy-$(CH_2)_4$-Sepharose (T=23°C, pH 7.0; time scale adjusted for a dead time of 187 s.

BSA adsorption on epoxy-$(CH_2)_4$-Sepharose, the measured enthalpy change of adsorption was at some conditions one to two orders of magnitude larger than the standard-state enthalpy change.

The concentration dependence of the enthalpy change of adsorption obtained from FMC was also shown to provide valuable insight on the adsorption of BSA on the Sepharose support. Using these data with adsorption isotherms. it has been argued that the confirmation of the adsorbed BSA plays an important role in determining the capacity of the sepharose support at high surface coverage.

5. Abbreviations

a, b, c	Parameters evaluated by least squares fitting for non-linear Van't Hoff analysis
ΔC_p	Heat capacity change
g_i	Concentration of component i in grams of i per gram of water
ΔH^0	Standard-state enthalpy change
ΔH_{ads}	Enthalpy change of adsorption
k'	Capacity factor
m_i	Molal concentration of component i
n	Total number of ions
R	Universal gas constant
ΔS^0	Standard-state entropy change
T_H	Reference temperature at which ΔH^0 is zero
T_S	Reference temperature at which ΔS^0 is zero

5.1. Greek symbols

ν_i	Moles of species *i* in the vicinity of the protein per mole of protein

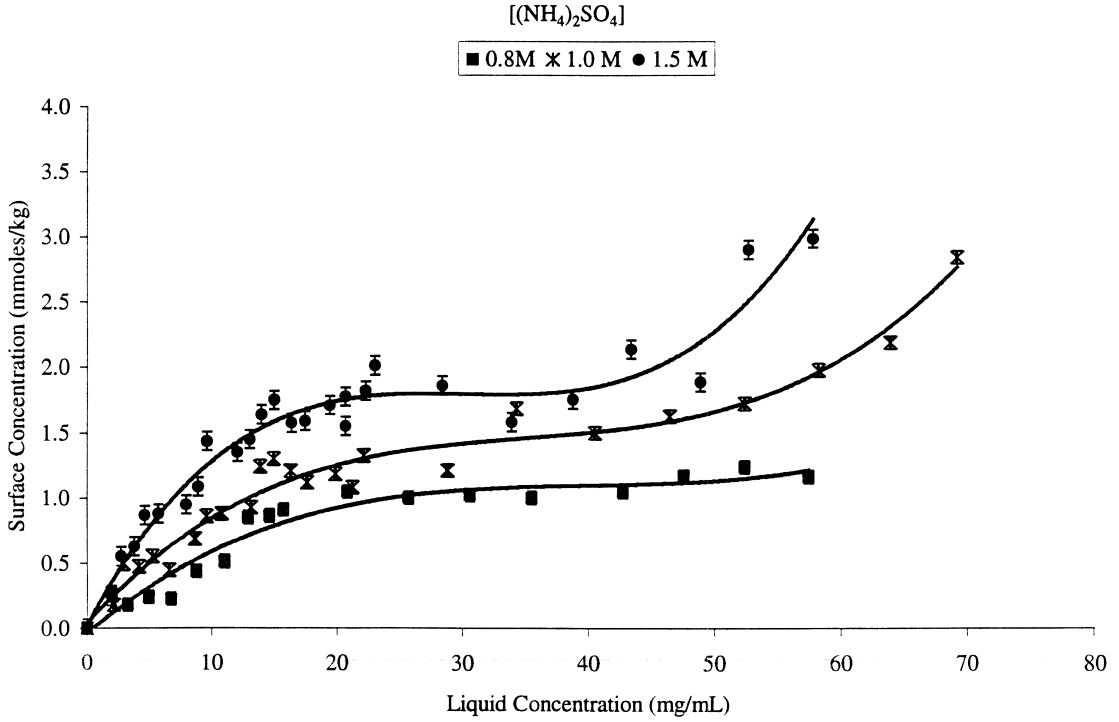

Fig. 9. Adsorption isotherms for BSA on epoxy-$(CH_2)_4$-Sepharose at $T=23°C$, pH = 7.0.

$\Delta\nu_i$	Stoichiometric weighted change in the number of moles
ϕ	Phase ratio

5.2. Subscripts

1	Water or solvent
2	Protein
3	Salt or solute
+	Cations
-	Anions

Acknowledgements

Two of the authors (M.E.K. and N.G.P) wish to acknowledge the helpful suggestions made by Professor Thatcher Root from the University of Wisconsin for the analysis of the FMC data.

References

[1] P. Gagnon, E. Grund, T. Lindback, Biopharm. (1995) 21–27.
[2] M. Einarsson, L. Kaplan, E. Nordenfelt, E. Miller, J. Virol. Methods 3 (1981) 213–228.
[3] J.A. Queiroz, F.A.P. Garcia, J.M.S. Cabral, J. Chromatogr. A 707 (1995) 137–142.
[4] M.E. Thrash, N.G. Pinto, in Encyclopedia of Analytical Chemistry, Wiley, New York, in press.
[5] M. Deutscher, Methods Enzymol. 182 (1990) 409–413.
[6] A. Vailaya, Cs. Horváth, Ind. Eng. Chem. Res. 35 (1996) 2964–2981.
[7] H. Dietmar, A. Vailaya, Cs. Horváth, Proc. Natl. Acad. Sci 93 (1996) 2290–2295.
[8] D.W. Lee, B.Y. Cho, Bull. Korean Chem. Soc. 14 (1993) 515–519.
[9] K. Kandori, M. Mukai, A. Fujiwara, T. Ishikawa, J. Colloid Interface Sci. 212 (1999) 600–603.
[10] T.W. Perkins, D.S. Mak, T.W. Root, E.N. Lightfoot, J. Chromatogr. A 766 (1997) 1–14.
[11] Microscal Origin Software Version 5.0, Microcal Software Inc., Northhampton, MA.
[12] Table Curve 2D Version 2.0, Jandel Scientific. AISN Software, 1989-1994.
[13] W. Norde, J. Lyklema, J. Colloid Interface Sci. 66 (1978) 257–265.